PHYSICAL REVIEW C VOLUME 31, NUMBER 6 JUNE 1985

Cluster picture of ^{7}Li

H. Walliser
Universität Tübingen, Institut für Theoretische Physik, 74 Tübingen, Federal Republic of Germany

T. Fliessbach
Universität-Gesamthochschule-Siegen, Fachbereich Physik, 59 Siegen, Federal Republic of Germany
(Received 14 December 1984)

The ^{7}Li nucleus is studied in a cluster picture with elementary alpha and triton particles as constituents. The relation of this elementary cluster model to the microscopic resonating group model is investigated. Within this cluster model various measurable quantities such as root mean square radii, transition probabilities, electromagnetic moments, and form factors are calculated and compared with the experiment. While the agreement for the electric quantities is surprisingly good, there are deviations for the magnetic ones.

I. INTRODUCTION

In physics there is no unique choice which particles should be treated as elementary ones in a model for describing and understanding the structure of matter. The choice of whether these particles are atoms, nuclei, nucleons, or quarks depends on the specific properties we want to describe. Consider the elastic form factor $F(q)$ for electron scattering. Clearly, in order to understand the diffraction pattern of electrons scattered from a crystal, one will treat nuclei as elementary particles. For $q \sim 0.1-1$ fm^{-1} the appropriate level is the level of nucleons, for higher q's the structure of nucleons has to be taken into account (including mesons or constructing a model with quarks as constituents).

The more fundamental or microscopic picture does not render the more macroscopic one obsolete or useless. Even if the most microscopic model can describe all properties the whole hierarchy of different levels is needed for understanding the structure of matter. To work with nucleons when describing electron scattering from a crystal obscures the physical understanding. Equally, no one will dismiss the n-p picture of the deuteron because he can handle the system on the quark level.

Nuclear physics has a tradition of treating nucleons as the elementary particles and this is certainly the appropriate level for a large domain of properties. But our understanding of nuclear structure has to be completed by embedding this level between the neighboring ones, the more and the less microscopic levels. For example, to understand the nucleon-nucleon interaction used as an ingredient for calculations on the nucleon level, we have to learn about the internal structure of the nucleons. On the other hand, collective modes in nuclei are not only described and understood on the nucleon level [e.g., by random-phase approximation (RPA) amplitudes] but also on the more macroscopic level of fluid dynamics. Again the point is that there is not only one exclusive microscopic level. Rather, the appropriate level depends on the properties considered and a full understanding is found in the hierarchy of different levels.

In this paper we want to investigate the possibility of a cluster picture for light nuclei as an intermediate level between the nucleus and the nucleon level. Instead of nucleons we consider stable configurations such as the α particle and the triton as constituents of the nucleus. In this context, we mean by cluster picture, a model treating the clusters as elementary (however not necessarily pointlike) particles, in a very similar way, as it is done for the nucleons in the nucleon picture of the deuteron.

A first indication about the possibility of such a cluster picture is given by the comparison of the mean distance $\langle R^2\rangle^{1/2}$ between the clusters and the sum of the cluster radii. The mean distance is deduced from the experimental root-mean-square (rms) radii of the two clusters (consisting of A and B nucleons) and that of the whole nucleus,

$$\langle r^2\rangle_{A+B} = \frac{A}{A+B}\langle r^2\rangle_A + \frac{B}{A+B}\langle r^2\rangle_B + \frac{AB}{(A+B)^2}\langle R^2\rangle \ . \tag{1}$$

The rms matter radii are estimated from the experimental rms charge radii of Barrett and Jackson[1] by correcting for the charge distributions of protons and neutrons. The geometrical situation is illustrated in Fig. 1 for some typical two-cluster systems.

There is a class of light nuclei, like ^{7}Li, ^{7}Be, ^{6}Li, ^{8}Be, and so on, in which the clusters forming these nuclei (α-t, α-^{3}He, α-d, α-α) are reasonably well separated. The difference between the nucleon picture for the deuteron and the cluster picture for these nuclei is not fundamental, only the exchange contributions are expected to be somewhat more important in the latter case because the clusters are closer to each other. With increasing mass number the two clusters begin to overlap and, in addition to larger exchange contributions, other channels will become more and more important. Then we can no longer expect one specific cluster configuration to be the dominant one. For the last example in Fig. 1, ^{32}S, even the microscopic

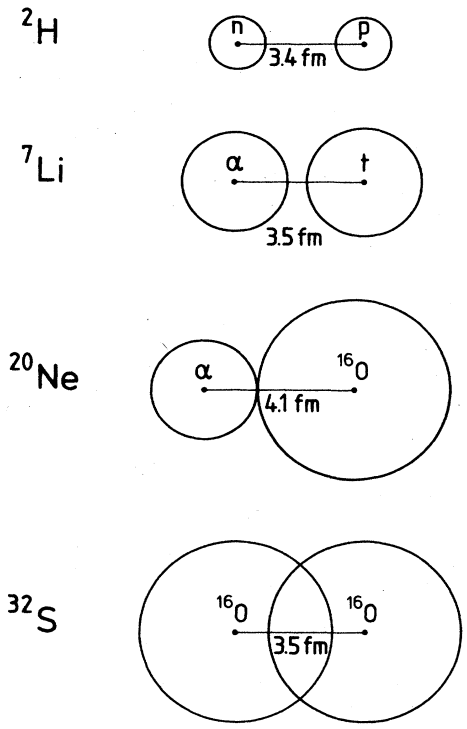

FIG. 1. Illustration of the size and mean separation of two clusters forming various nuclei. The cluster sizes are taken from Ref. 1. The intercluster distance is calculated with Eq. (1).

two-cluster picture[2] (including Pauli distortions) cannot describe the ground state.

The pictures in Fig. 1 are, however, only a first indication about the validity of a cluster picture: A large $\langle R^2 \rangle$ in Eq. (1) does not necessarily imply that the system behaves like a two cluster system. Furthermore, even if the system may be described in this way there might exist substantial polarization effects also for well-separated clusters. Contrarily, for overlapping clusters there might still be a domain of properties not altered much by the mutual distortion.

For a more profound discussion we choose ^{7}Li as an example, which according to Fig. 1 might be a good candidate for an elementary cluster picture. ^{7}Li has the advantage that many experimental data are available. Furthermore, there are a number of successful microscopic (nucleon level) calculations. We investigate the following questions for ^{7}Li:

(i) Is the elementary cluster picture adequate for this system? More specifically we determine the domain of properties which may be explained and thus understood on this level. The question is then: Is this domain sufficiently large to justify the introduction of this level (maybe with a similar degree of justification as the n-p description of the deuteron)?

(ii) What is the connection to the next more fundamental level, the nucleon picture? In view of existing calculations[3–5] which successfully describe many properties of ^{7}Li this might seem trivial because we have only to go from the more microscopic level to the less microscopic one. The unique answer to the question posed is, however, nontrivial.

The ultimate check of the validity of any specific model lies in its ability to reproduce the experimental data. Therefore the validity of the cluster model for ^{7}Li will be examined by the investigation of question (i). For this step the availability of a microscopic resonating group method (RGM) calculation is not required. However, the investigation of (ii) is useful because it completes the physical understanding by embedding the cluster picture into the more fundamental level.

II. DEFINITION OF THE CLUSTER PICTURE

We define now the model in which ^{7}Li is treated as a system composed by an elementary α particle plus an elementary triton (t). For this purpose we have to specify the *wave function* and the *operators* from which the observables may be calculated.

The relative motion of the clusters in the ground state will be described by a bound state wave function $\psi(\mathbf{R})$ with

$$\int d\mathbf{R}\,|\psi(\mathbf{R})|^2=1, \quad \mathbf{R}=\mathbf{R}_\alpha-\mathbf{R}_t\,, \tag{2}$$

where $\mathbf{R}_\alpha$ and $\mathbf{R}_t$ denote the position of the clusters. This wave function may be determined by one of the following possibilities:

(i) ψ is considered as a quantity to be determined by the experiment. In particular, the form factor for elastic electron scattering yields basically the Fourier transform of $|\psi|^2$.

(ii) ψ is calculated as the solution of a one-body Schrödinger equation with an effective α-t potential.

(iii) ψ is derived from a microscopic wave function $\Psi(\mathbf{r}_1, \ldots, \mathbf{r}_7)$ describing the system on the nucleon level.

All these possibilities require to some extent the validity of the elementary cluster picture. Our investigation will show to which extent the resulting picture is a consistent one.

In this paper we will discuss only the possibilities (i) and (iii). The possibility (ii) was, for example, successfully applied to the description of the ^{3}He$(\alpha,\gamma)^7$Be and ^{2}H$(\alpha,\gamma)^6$Li capture reactions.[6] In this direct capture model the bound state wave function ψ (and similarly the continuum wave functions) is calculated from an effective potential fitted to the low energy scattering data. This procedure is well known for the deuteron where the effective nucleon-nucleon interaction deduced from the scattering data can be profitably employed to other systems as well. In our case however, the detour about an effective potential is not too much of an advantage.

As stated above we treat the α and t as elementary particles, that means we do not allow for distortions of the clusters. Without leaving the elementary cluster picture we will, however, take into account the finite size of the clusters. We remember here that the finite size of the nucleons is introduced in calculations on the nucleon level simply by folding the operators in question with the proton and neutron internal densities. As an example let us

consider the charge form factor operator

$$\mathscr{M}=\frac{1}{Z}\sum_{j=1}^{A} F^{\mathrm{ch}}_{\tau_j}(\mathbf{q})e^{i\mathbf{q}(\mathbf{r}_j-\mathbf{R}_{\mathrm{c.m.}})} . \tag{3}$$

The finite sizes of the nucleons enter simply via the proton and neutron charge form factors

$$F^{\mathrm{ch}}_{\mathrm{p,n}}(\mathbf{q})=\int d\mathbf{r}\rho^{\mathrm{ch}}_{\mathrm{p,n}}(\mathbf{r})\exp(i\mathbf{qr})$$

($\rho^{\mathrm{ch}}_{\mathrm{p,n}}$ are the internal charge densities of the proton and the neutron, respectively).

Using the analogous procedure in the elementary cluster picture, we have to fold over the internal cluster densities given by the undisturbed internal wave functions ϕ_α and ϕ_{t}:

$$\begin{aligned} m(\mathbf{R})&=\int d\xi\,|\phi_\alpha|^2|\phi_{\mathrm{t}}|^2\mathscr{M} ,\\ &=\tfrac{2}{3}F^{\mathrm{ch}}_\alpha(\mathbf{q})e^{(3/7)i\mathbf{qR}}+\tfrac{1}{3}F^{\mathrm{ch}}_{\mathrm{t}}(\mathbf{q})e^{-(4/7)i\mathbf{qR}} . \end{aligned} \tag{4}$$

The integration $d\xi$ runs over the internal coordinates of α and t. Here, we restricted the operator $\mathscr{M}$ to be local, resulting in a local cluster operator $m(\mathbf{R})$. As in the nucleon case, the finite sizes of the clusters enter for our example simply via the α and t charge form factors $F^{\mathrm{ch}}_\alpha(\mathbf{q})$ and $F^{\mathrm{ch}}_{\mathrm{t}}(\mathbf{q})$.

In general, the operator $\mathscr{M}$ may contain derivatives (specifically angular momentum operators). For this case the folding procedure (4) is generalized defining the cluster operator $\hat{m}$ by

$$\begin{aligned} \langle\mathbf{R}|\hat{m}|\mathbf{R}'\rangle&=\langle\delta(\mathbf{R}-\mathbf{R}_{\alpha\mathrm{t}})\phi_\alpha\phi_{\mathrm{t}}|\mathscr{M}|\delta(\mathbf{R}'-\mathbf{R}_{\alpha\mathrm{t}})\phi_\alpha\phi_{\mathrm{t}}\rangle ,\\ &=\delta(\mathbf{R}-\mathbf{R}')\int d\xi\,\phi^*_\alpha\phi^*_{\mathrm{t}}\mathscr{M}\phi_\alpha\phi_{\mathrm{t}} ,\\ &=m(\mathbf{R},\nabla_{\mathbf{R}})\delta(\mathbf{R}-\mathbf{R}') . \end{aligned} \tag{5}$$

The definition (5) is a unique prescription for the consideration of the finite size effects. In the elementary cluster picture the microscopic wave functions ϕ_α and ϕ_{t} are not needed. As in Eq. (4), they are replaced by the experimental form factors and rms radii. Thus the cluster model is handled in a consistent way without reference to the internal wave functions.

Note that the cluster operator $\hat{m}$ is *not* defined as the effective (in general complicated) operator yielding the same expectation values as $\mathscr{M}$, but simply as the operator that one would naively use for elementary but extended particles.

III. RELATION BETWEEN THE ELEMENTARY AND THE MICROSCOPIC CLUSTER PICTURE

In order to connect the cluster and the nucleon level we have to establish the relation between the corresponding *wave functions* and the operators or, more specifically, the *expectation values* of the operators.

The elementary cluster picture is strongly motivated by the success of the microscopic cluster model.[3–5] The microscopic cluster model wave function Ψ depends on all nucleon coordinates and is for ^{7}Li of the form

$$\Psi(^7\mathrm{Li})=\mathscr{A}u(\mathbf{R}_{\alpha\mathrm{t}})\phi_\alpha\phi_{\mathrm{t}} . \tag{6}$$

Here $\mathscr{A}$ denotes the antisymmetrization operator and $\mathbf{R}_{\alpha\mathrm{t}}$ the relative coordinate of α and t. For clarity in representation we omit all angular momentum indices, knowing that the spin $\frac{1}{2}$ of the triton may couple with the orbital angular momentum 1 of the relative motion function u, to the total angular momenta $(\frac{3}{2})^-$ for the ^{7}Li ground state, and to $(\frac{1}{2})^-$ for the first excited state ^{7}Li*. This first excited state at 0.478 MeV can be described by the same ansatz (6). In particular, we refer to the single channel resonating group method (RGM) calculation of Kanada *et al.*,[3] where the internal wave functions ϕ_α and ϕ_{t} were represented by simple $(1s)^4$ and $(1s)^3$ configurations in harmonic oscillator wells whose widths, $\alpha=0.514$ fm^{-2} and $\beta=0.378$ fm^{-2}, were chosen differently. The RGM function $u(\mathbf{R})$ is variationally determined by minimizing the expectation value of the many-body Hamiltonian with a realistic nucleon-nucleon force, including a spin-orbit part.

In contrast to the elementary cluster picture, the ansatz (6) is a description on the nucleon level. Although undisturbed wave functions $(\phi_\alpha,\phi_{\mathrm{t}})$ for the clusters are used, distortions due to the antisymmetrization are taken into account (Pauli distortions). The success of the microscopic cluster model in explaining the properties of ^{7}Li implies that Eq. (6) is a good approximation for the microscopic wave function (ground state and first excited state). Therefore, we take Eq. (6) as the appropriate description of ^{7}Li on the nucleon level and investigate its relation to the elementary cluster picture. The first step is the reduction of the many-body wave function Ψ to the cluster wave function ψ of Eq. (2). For this purpose we rewrite Eq. (6) in the following equivalent forms:

$$\begin{aligned} |\Psi(^7\mathrm{Li})\rangle&=\int d\mathbf{R}\,u(\mathbf{R})\,|\mathscr{A}\delta(\mathbf{R}-\mathbf{R}_{\alpha\mathrm{t}})\phi_\alpha\phi_{\mathrm{t}}\rangle ,\\ &=\int d\mathbf{R}\,\omega(\mathbf{R})\,|\mathscr{A}N^{-1/2}\delta(\mathbf{R}-\mathbf{R}_{\alpha\mathrm{t}})\phi_\alpha\phi_{\mathrm{t}}\rangle ,\\ &=\int d\mathbf{R}\,y(\mathbf{R})\,|\mathscr{A}N^{-1}\delta(\mathbf{R}-\mathbf{R}_{\alpha\mathrm{t}})\phi_\alpha\phi_{\mathrm{t}}\rangle . \end{aligned} \tag{7}$$

The norm of the basis states of $u(\mathbf{R})$ defines the nonlocal norm kernel N (often denoted by $1-\hat{K}$),

$$\begin{aligned} N(\mathbf{R},\mathbf{R}')&=(1-\hat{K})_{\mathbf{R},\mathbf{R}'}\\ &=\langle\mathscr{A}\delta(\mathbf{R}-\mathbf{R}_{\alpha\mathrm{t}})\phi_\alpha\phi_{\mathrm{t}}\,|\,\mathscr{A}\delta(\mathbf{R}'-\mathbf{R}_{\alpha\mathrm{t}})\phi_\alpha\phi_{\mathrm{t}}\rangle . \end{aligned} \tag{8}$$

In Eq. (7) there are three candidates (u, ω, or y) for the intercluster wave function ψ of Eq. (2). Since ψ is a wave function in the elementary cluster picture it has the meaning of a probability amplitude. The functions u, ω, and y in Eq. (6) are weight functions of basis states normalized to $N(\mathbf{R},\mathbf{R}')$, $\delta(\mathbf{R}-\mathbf{R}')$, and $N^{-1}(\mathbf{R},\mathbf{R}')$, respectively. Therefore, only $\omega(\mathbf{R})$ has a possible interpretation as a probability amplitude,[7] namely the probability of finding the antisymmetrized and normalized cluster state with parameter $\mathbf{R}$ in Ψ. Therefore, among the three functions u, ω, or y, the only possible and consistent identification is

$$\psi(\mathbf{R})=\omega(\mathbf{R}) . \tag{9}$$

The radial parts of the functions u, ω, and y are shown in Fig. 2 for the ^{7}Li ground state (those for the first excited state look quite similar). The strange behavior of $u(\mathbf{R})$ in the interior is due to the existence of a small eigenvalue

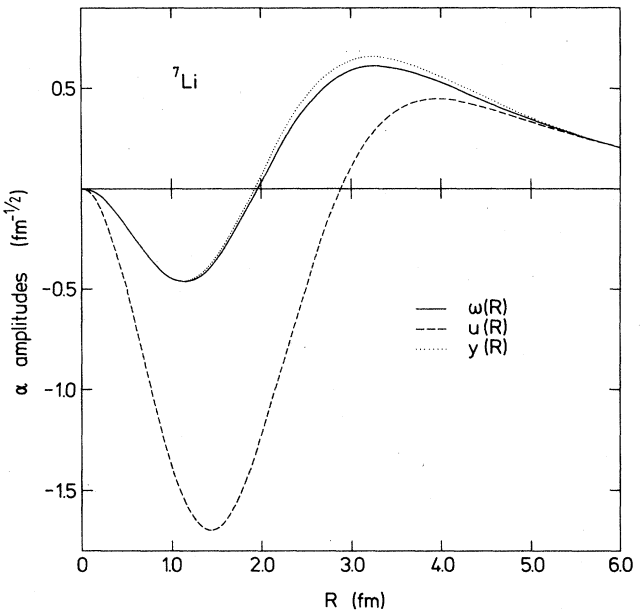

FIG. 2. Radial part of the α amplitudes ω, u, and y for the ^{7}Li ground state.

of the norm kernel (almost forbidden state). The relative smallness of the difference between ω and y is a special feature of the α-t system where the eigenvalues of the norm kernel do not deviate much from 1 (apart from the almost forbidden state). For physical quantities (in particular the rms radius, see below) y and ω lead, however, to distinctly different results. Compared to ω the amplitude y overestimates the amount of α clustering in the surface.

For large $R=|\mathbf{R}|$, where the clusters do not overlap and the antisymmetrization in Eq. (6) does not lead to distortions, the interpretation of $\omega(\mathbf{R})$ and $\psi(\mathbf{R})$ is obvious, namely the probability amplitude of finding the clusters at distance R. The crucial region is the interior ($R \lesssim 4$ fm) where the two clusters may have some overlap and their structures may be distorted by antisymmetrization. Here $\omega(\mathbf{R})$ is not a quantity which can be measured directly. There are, however, a number of physical quantities which depend strongly on the interior ($R \lesssim 4$ fm) of the wave function. Then the identification (9) is valid to the degree to which these quantities can be calculated in the elementary cluster picture with ψ. For an arbitrary observable with the operator $\mathcal{M}$ this means that we have to investigate the approximation

$$\langle \Psi(^7\mathrm{Li}) | \mathcal{M} | \Psi(^7\mathrm{Li}) \rangle \simeq \langle \omega | \hat{m} | \omega \rangle \tag{10}$$

with the corresponding cluster operator (5). We will find that this approximation holds for a number of physical properties. Within the range of these properties the elementary cluster model is then of the same validity as the underlying microscopic model (6).

The first candidate for testing Eq. (10) is the matter radius. The expectation value of the operator,

$$\mathcal{M} = \frac{1}{A} \sum_{i=1}^{A} (\mathbf{r}_i - \mathbf{R}_{\mathrm{c.m.}})^2 \tag{11}$$

TABLE I. Normalization and intercluster rms radii calculated for various α amplitudes. The calculated rms radii have to be compared to the exact RGM value $\langle R^2 \rangle_{\mathrm{RGM}} = 13.98$ fm^2.

Normalization	Intercluster mean square radius
$\langle u \mid u \rangle = 3.76$	$\langle u \mid R^2 \mid u \rangle = 17.13$ fm^2
$\langle \omega \mid \omega \rangle = 1$	$\langle \omega \mid R^2 \mid \omega \rangle = 13.86$ fm^2
$\langle y \mid y \rangle = 1.11$	$\langle y \mid R^2 \mid y \rangle = 15.22$ fm^2
$\langle u \mid y \rangle = 1$	$\langle u \mid R^2 \mid y \rangle = 10.89$ fm^2
	$\frac{\langle u \mid R^2 \mid u \rangle}{\langle u \mid u \rangle} = 4.56$ fm^2
	$\frac{\langle y \mid R^2 \mid y \rangle}{\langle y \mid y \rangle} = 13.77$ fm^2

leads to Eq. (1) with a value $\langle R^2 \rangle_{\mathrm{RGM}}$ for the left-hand side (lhs) of Eq. (10) and $\langle R^2 \rangle = \langle \omega \mid R^2 \mid \omega \rangle$ for the right-hand side (rhs) of Eq. (10) (the contributions of the clusters themselves are the same on both sides). The resulting values are (see Table I) 13.98 and 13.86 fm^2, respectively.

At this point we repeated the calculation for the inconsistent identifications $\psi = u$ and $\psi = y$. The results are shown in Table I. Even after an overall normalization ($\psi = u/\langle u \mid u \rangle^{1/2}$ and $\psi = y/\langle y \mid y \rangle^{1/2}$) the (consistent) identification (9) is favored.

It may be mentioned that Eq. (10) becomes exact in an analytical model[8] with the following three characteristics:

(i) ϕ_α, ϕ_t are oscillator functions with the same oscillator width ($\alpha = \beta$).

(ii) $\omega(\mathbf{R})$ is an oscillator function corresponding to the same frequency.

(iii) $\mathcal{M}$ is the kinetic energy operator, the operator (11), or the quadrupole operator.

For matrix elements between oscillator states of different energy the lhs of Eq. (10) can be exactly reduced to $\langle u \mid m \mid y \rangle$ in this analytical model. This form has been proposed in Ref. 9 also for more general operators. In the present case this expression yields, however, a considerably worse result (Table I). The reason for this is that the derivations in the analytical model refer to the equal frequency ($\alpha = \beta$) case. In the present calculation ($\alpha \neq \beta$) it is just the contribution of the state which is forbidden for $\alpha = \beta$ which leads to the strange behavior of u (Fig. 1).

We restrict now the discussion to $\psi = \omega$. Then the cluster picture results [rhs of Eq. (10)] are compared in Table II to the exact RGM results [lhs of Eq. (10)]. The approximation (10) is excellent for pure matter quantities and becomes little worse for quantities involving the charges. Exchanges of protons and neutrons affect the latter quantities more sensitively. Still, from Table II we conclude: The reduction of the microscopic cluster model to the elementary cluster model is a good approximation provided that the wave function of the clusters is identified with ω.

For the elastic form factor of ^{7}Li this elementary clus-

TABLE II. Comparison between the results of the elementary cluster model and the microscopic cluster model (RGM, Refs. 3 and 5) for various properties of ^{7}Li. The finite size effects of the individual elementary clusters is calculated with the undisturbed wave functions ϕ_α and ϕ_t.

Physical quantity	Elementary cluster model	RGM
$\langle r^2\rangle^{\text{matter } 1/2}$ (fm)	2.40	2.41
Q^{matter} (fm^2)	−4.07	−4.11
$\langle r^2\rangle^{\text{ch } 1/2}$ (fm)	2.47	2.44
Q^{elect} (fm^2)	−3.85	−3.70
$\mu^{\text{mag}}(\mu_N)$	3.20	3.15
$B(M1;\frac{3}{2}\to\frac{1}{2})$ (μ_N^2)	2.13	2.17
$B(C2;\frac{3}{2}\to\frac{1}{2})$ $(e^2\text{fm}^4)$	8.04	7.55

ter model has already been used by Liu *et al.*[10] They found satisfactory agreement with the exact RGM results in the low q^2 region. In the squared form factor the error is less than 4% for $q^2<4$ fm^{-2}. The higher q^2 are more sensitive to the region where the clusters overlap more strongly and the approximation becomes less accurate.

Altogether, the comparison with the microscopic calculations indicates that the elementary cluster model for ^{7}Li is quite reasonable.

IV. PHYSICAL PROPERTIES IN THE CLUSTER PICTURE

A. Model input

In this section we will calculate various properties of ^{7}Li in the elementary cluster picture and compare the results with experimentally determined values. For this purpose we need the *cluster wave function* ψ and the *operators* $\hat{m}$ corresponding to the considered observables.

The form factors and rms radii of the individual clusters enter into the expressions for the operators $\hat{m}$ [compare Eq. (4)]. These quantities are taken from the experiment[11] as an input for the model. In this way the finite size of the otherwise elementary clusters is taken into account.

The intercluster wave function ψ may be determined in principle from the elastic form factor. In this way we can treat ^{7}Li consistently on the level of the elementary cluster picture without reference to microscopic quantities. As discussed below in Sec. IV C, the determination of ψ from the elastic form factor will yield a function which is very similar to the ω function of a RGM calculation. In view of the availability of these ω functions we fixed the cluster wave function ψ for the ground state $[(\frac{3}{2})^-]$ and for the first excited state $[(\frac{1}{2})^-]$ by

$$\psi_{3/2}(\mathbf{R})=\omega_{3/2}(\mathbf{R}),\quad \psi_{1/2}(\mathbf{R})=\omega_{1/2}(\mathbf{R})\ . \tag{12}$$

We emphasize once more that we use the results of existing RGM calculations for ψ only for convenience; the elementary cluster model itself does not require such a calculation.

B. Longitudinal form factor

The longitudinal form factor for ^{7}Li

$$|F_L(q)|^2=|F_{C0}(q)|^2+|F_{C2}(q)|^2+|F'_{C2}(q)|^2 \tag{13}$$

contains the $C0$ and $C2$ contributions from elastic scattering and the $C2'$ contribution from scattering to the first excited state ^{7}Li*. The individual form factors

$$F_{C\lambda}(q)=\frac{\sqrt{\pi}}{3e}\frac{q^\lambda}{(2\lambda+1)!!}\langle J_i||\mathscr{M}(C\lambda,q)||J_f\rangle \tag{14}$$

are expressed by the reduced matrix elements of the multipole operators $\mathscr{M}(C\lambda,\mu,q)$, given explicitly by Willey.[12] In the elementary cluster model the form factors are approximated by one-body matrix elements,

$$F_{C\lambda}(q)\simeq\frac{\sqrt{\pi}}{3e}\frac{q^\lambda}{(2\lambda+1)!!}\langle\psi_{J_i}||m(C\lambda,q)||\psi_{J_f}\rangle\ , \tag{15}$$

with the cluster operators

$$m(C\lambda,\mu,q)=e\frac{(2\lambda+1)!!}{q^\lambda}\left[\tfrac{2}{3}F_\alpha^{\text{ch}}(q)j_\lambda(\tfrac{3}{7}qR)+\tfrac{1}{3}F_t^{\text{ch}}(q)j_\lambda(\tfrac{4}{7}qR)\right]Y_{\lambda\mu}(\hat{\mathbf{R}}) \tag{16}$$

corresponding to the multipole operators $\mathscr{M}(C\lambda,\mu,q)$. This is just the example given in Eqs. (3) and (4) for a definite multipole λ (j_λ is a spherical Bessel function, $Y_{\lambda\mu}$ are spherical harmonics). The form factors (15),

$$\begin{aligned}F_{C0}(q)&=\tfrac{2}{3}F_\alpha^{\text{ch}}(q)F_0(\tfrac{3}{7}q)+\tfrac{1}{3}F_t^{\text{ch}}(q)F_0(\tfrac{4}{7}q)\ ,\\ F_{C2}(q)&=-\tfrac{2}{3}F_\alpha^{\text{ch}}(q)F_2(\tfrac{3}{7}q)-\tfrac{1}{3}F_t^{\text{ch}}(q)F_2(\tfrac{4}{7}q)\ ,\\ F'_{C2}(q)&=\tfrac{2}{3}F_\alpha^{\text{ch}}(q)F'_2(\tfrac{3}{7}q)+\tfrac{1}{3}F_t^{\text{ch}}(q)F'_2(\tfrac{4}{7}q)\ ,\end{aligned} \tag{17}$$

are then expressed very simply by the "form factors" F_0, F_2, and F'_2 of the intercluster wave functions:

$$\begin{aligned}F_\lambda(q)&\equiv\langle\tilde{\psi}_{3/2}|j_\lambda|\tilde{\psi}_{3/2}\rangle\ ,\\ F'_\lambda(q)&\equiv\langle\tilde{\psi}_{3/2}|j_\lambda|\tilde{\psi}_{1/2}\rangle\ .\end{aligned} \tag{18}$$

Here we introduced the radial part $\tilde{\psi}$ of ψ,

$$\psi(\mathbf{R})=Y_{1m}(\hat{\mathbf{R}})\tilde{\psi}(R)/R\ . \tag{19}$$

Equations (17) and (18) are the final expressions for the longitudinal form factors in the elementary cluster picture. The calculated $C0$, $C2$, and $C2'$ contributions are shown in Fig. 3. Their sum is compared to the experimental longitudinal form factor of Suelzle *et al.*,[13] extracted from their measured total cross section by subtracting a best fit to the magnetic scattering data of Rand *et al.*[14] There is excellent agreement between the calculated and experimental values over the whole q^2 region plotted in Fig. 3. For the longitudinal form factor the elementary cluster picture is thus a surprisingly accurate model.

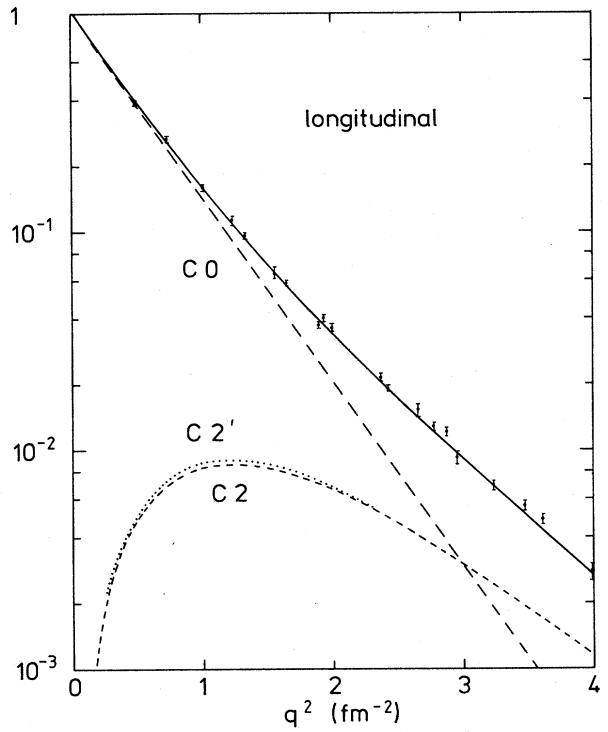

FIG. 3. Longitudinal form factor for ^{7}Li (solid line) containing the elastic $C0$ and $C2$ contributions (dashed lines) and the inelastic $C2'$ transition to the first excited ^{7}Li* state at 0.478 MeV (dotted line), calculated in the elementary cluster model. The experimental data are from Ref. 13.

C. Determination of the cluster wave function from experiment

As mentioned in Sec. IV A the intercluster wave function ψ should in principle be determined by the experiment in order to treat the model consistently on the cluster level. We discuss now this determination in some detail for the ^{7}Li ground state. To simplify the situation we start with the experimental elastic charge form factor for ^{7}Li of Suelzle *et al.*,[13]

$$|F_{ch}(q)|^2 = |F_{C0}(q)|^2 + |F_{C2}(q)|^2 \tag{20}$$

containing the $C0$ and $C2$ contribution only (the $C2'$ contribution is substracted in a slightly model dependent way). From this experimental information (20), we obtain the wanted function $|\tilde{\psi}_{3/2}(R)|^2$ by unfolding Eqs. (17) and (18).

There is one practical difficulty in this procedure. The reproduction of Eq. (18) also for high q's ($q \gg k_F$, where k_F is the Fermi momentum) forces the Fourier transform of $|\tilde{\psi}_{3/2}(R)|^2$ to simulate effects which are completely outside the scope of the considered model. Depending on the high q behavior of $F_{ch}(q)$, $F_\alpha^{ch}(q)$, and $F_t^{ch}(q)$, this might lead to an unphysical result for $|\tilde{\psi}_{3/2}(R)|^2$, especially to a violation of the condition $|\tilde{\psi}_{3/2}(R)|^2 \geq 0$.

The proper remedy to this difficulty is the restriction to low q values ($q \lesssim k_F$, for example $q < 2$ fm^{-1}). In practice this can be achieved by expanding $\psi_{3/2}$ into a number of suitable basis states. The expansion coefficients can then be determined by fitting the form factor in the low q region. A successful fit requires, naturally, a sensible choice of the basis states.

There will exist a family of wave functions ψ which fulfill the criteria stated above but which may show small deviations stemming from the high q components. The function $\omega_{3/2}$ of the microscopic RGM calculation is also a member of this family because it fits the experimental charge form factor quite accurately for $q < 2$ fm^{-1}. Thus we may alternatively regard this $\omega_{3/2}$ as the function ψ deduced from the experiment. It should be noted that the calculated physical quantities considered here depend only weakly on the uncertainty in the high q components of ψ.

D. Transverse form factor

The transverse form factor includes the elastic $M1$ and $M3$ contributions and the inelastic $M1'$ and $E2'$ contributions

$$|F_T(q)|^2 = |F_{M1}(q)|^2 + |F_{M3}(q)|^2 + |F'_{M1}(q)|^2 + |F'_{E2}(q)|^2 . \tag{21}$$

The individual form factors related to the multipole operators $\mathcal{M}(M\lambda,\mu,q)$ and $\mathcal{M}(E\lambda,\mu,q)$ (Ref. 12)

$$F_{M(E)\lambda}(q) = \left[\frac{9\pi(\lambda+1)}{10\lambda}\right]^{1/2} \frac{q^{\lambda-1}}{(2\lambda+1)!!\mu^{\text{mag}}} \langle J_i||\mathcal{M}[M(E)\lambda,q]||J_f\rangle \simeq \left[\frac{9\pi(\lambda+1)}{10\lambda}\right]^{1/2} \frac{q^{\lambda-1}}{(2\lambda+1)!!\mu^{\text{mag}}}$$
$$\times \langle \psi_{J_i}||m[M(E),\lambda,q]||\psi_{J_f}\rangle , \tag{22}$$

are again approximated by one-body matrix elements involving the corresponding cluster operators

$$m(M\lambda,\mu,q) = \frac{2\mu_N}{\lambda+1} \frac{(2\lambda+1)!!}{q^{\lambda-1}}$$
$$\times \left\{ \tfrac{3}{14} F_\alpha^{ch}(q) \left[\left[\frac{\lambda+1}{2\lambda+1}\right]^{1/2} j_{\lambda+1}(\tfrac{3}{7}qR) Y_{\lambda\lambda+1\mu}(\hat{\mathbf{R}}) + \left[\frac{\lambda}{2\lambda+1}\right]^{1/2} j_{\lambda-1}(\tfrac{3}{7}qR) Y_{\lambda\lambda-1\mu}(\hat{\mathbf{R}}) \right] \mathbf{L} \right.$$

$$+\tfrac{4}{21}F_t^{ch}(q)\left[\left[\frac{\lambda+1}{2\lambda+1}\right]^{1/2} j_{\lambda+1}(\tfrac{4}{7}qR)\mathbf{Y}_{\lambda\lambda+1\mu}(\hat{\mathbf{R}})+\left[\frac{\lambda}{2\lambda+1}\right]^{1/2} j_{\lambda-1}(\tfrac{4}{7}qR)\mathbf{Y}_{\lambda\lambda-1\mu}(\hat{\mathbf{R}})\right]\mathbf{L}$$

$$-\frac{g_t}{2}F_t^{mag}(q)\left[\lambda\left[\frac{\lambda+1}{2\lambda+1}\right]^{1/2} j_{\lambda+1}(\tfrac{4}{7}qR)\mathbf{Y}_{\lambda\lambda+1\mu}(\hat{\mathbf{R}})-(\lambda+1)\left[\frac{\lambda}{2\lambda+1}\right]^{1/2} j_{\lambda-1}(\tfrac{4}{7}qR)\mathbf{Y}_{\lambda\lambda-1\mu}(\hat{\mathbf{R}})\right]\mathbf{S}\Bigg\} \tag{23}$$

$$m(E\lambda,\mu,q)=\frac{2\mu_N}{\lambda+1}\frac{(2\lambda+1)!!}{q^{\lambda-1}}\frac{g_t}{2}F_t^{mag}(q)\sqrt{\lambda(\lambda+1)}j_\lambda(\tfrac{4}{7}qR)\mathbf{Y}_{\lambda\lambda\mu}(\hat{\mathbf{R}})\mathbf{S}\ .$$

In Eq. (23) F_t^{mag} is the triton magnetic form factor, g_t is the triton g factor, and $\mu_N=e\hbar/2mc$ is the nuclear magneton. Equation (23) involves, further, the vector spherical harmonics $\mathbf{Y}$, the orbital angular momentum $\mathbf{L}$ of the α-t relative motion, and the spin $\mathbf{S}$ of the triton. The magnetic moment μ^{mag} of ^{7}Li appearing in Eq. (22) is also calculated in the α-t cluster model (see below). For the calculation of $m(E\lambda,\mu,q)$ two less important terms in $\mathcal{M}(E\lambda,\mu,q)$ leading to only small corrections were omitted. From Eqs. (22) and (23) we obtain

$$F_{M1}(q)=\frac{\mu_N}{\mu^{mag}}\left\{\tfrac{3}{14}F_\alpha^{ch}(q)[F_0(\tfrac{3}{7}q)+F_2(\tfrac{3}{7}q)]+\tfrac{4}{21}F_t^{ch}(q)[F_0(\tfrac{4}{7}q)+F_2(\tfrac{4}{7}q)]+\frac{g_t}{2}F_t^{mag}(q)[F_0(\tfrac{4}{7}q)-\tfrac{1}{5}F_2(\tfrac{4}{7}q)]\right\},$$

$$F_{M3}(q)=-\frac{\mu_N}{\mu^{mag}}\frac{3}{5}\sqrt{3/2}g_tF_t^{mag}(q)F_2(\tfrac{4}{7}q)\ , \tag{24}$$

$$F'_{M1}(q)=\frac{\mu_N}{\mu^{mag}}\frac{1}{\sqrt{5}}\{-\tfrac{3}{14}F_\alpha^{ch}(q)[F'_0(\tfrac{3}{7}q)+F'_2(\tfrac{3}{7}q)]-\tfrac{4}{21}F_t^{ch}(q)[F'_0(\tfrac{4}{7}q)+F'_2(\tfrac{4}{7}q)]+g_tF_t^{mag}(q)[F'_0(\tfrac{4}{7}q)+\tfrac{1}{4}F'_2(\tfrac{4}{7}q)]\}\ ,$$

$$F'_{E2}(q)=-\frac{\mu_N}{\mu^{mag}}\frac{3}{4}\sqrt{3/5}g_tF_t^{mag}(q)F'_2(\tfrac{4}{7}q)\ .$$

Together with Eq. (18) for the relative motion form factors, Eq. (24) is the result for the transverse form factor in the elementary cluster model. The experimental form factors for the individual clusters (consistent with a value $g_t=5.958$ for the triton g factor) are again used as an input of the calculation.

The calculated $M1$, $M3$, $M1'$, and $E2'$ contributions are depicted in Fig. 4. Their sum is compared with the experimental data of Rand *et al.*[14] As is seen from Fig. 4 the calculated form factor comes out much too low in the higher q^2 region. Especially, the diffraction minimum in the $M1$ contribution at $q^2\simeq 2$ fm^{-2}, obtained in exact RGM or generator coordinate method calculations,[4] is not seen in the cluster model (the same is also true for a diffraction minimum in the electric $C0$ contribution, which appears, however, in a q^2 region, $q^2\simeq 6$–7 fm^{-2}, of not much importance).

Due to the missing diffraction minima in the dominant $M1$ and $M1'$ contributions around $q^2\simeq 2$ fm^{-2}, the transverse form factor is not well described by the elementary cluster model in the higher q^2 region. In this model only the triton carries a spin and the α particle does not at all contribute to the dominant spin-dependent parts of magnetic multipole operators. This seems to be a very rough picture considering that from the microscopic point of view all seven nucleons carry a spin and contribute to the spin parts of the magnetic form factors.

With concern to the diffraction minimum, a similar phenomenon is observed in the ^{3}He charge form factor. There the diffraction minima around $q^2\simeq 11$ and 70 fm^{-2} are not understood on the nucleon level. To get their ex-

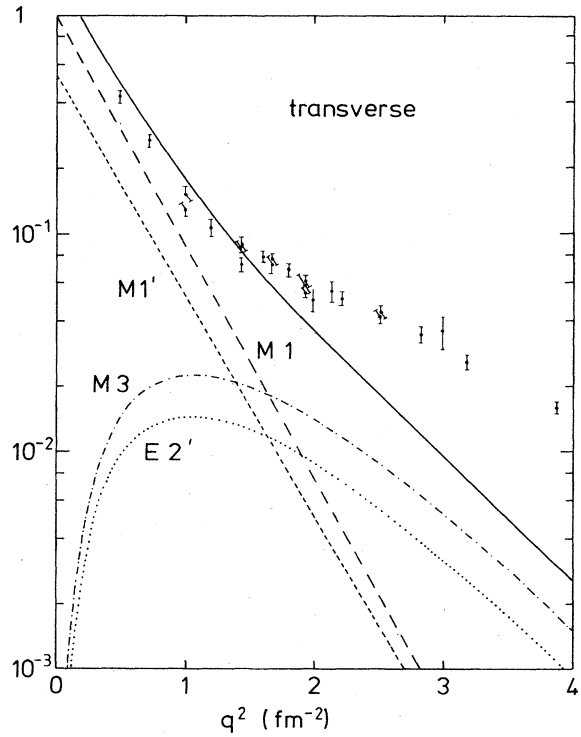

FIG. 4. Transverse form factor for ^{7}Li (solid line) containing the elastic $M1$ and $M3$ contributions (dashed) and the inelastic $M1'$ and $E2'$ contributions (dotted), calculated in the elementary cluster picture. The experimental data are taken from Ref. 14.

TABLE III. Comparison between calculated (elementary cluster model) and experimental values for various properties of ^{7}Li. The finite size effects of the individual elementary clusters are taken from the experiment via the corresponding rms radii of the single clusters.

Physical quantity	Elementary cluster model	Experiment	
$\langle r^2\rangle^{\mathrm{ch}\ 1/2}$ (fm)	2.46	2.55±0.07	(Ref. 15)
		2.39±0.03	(Ref. 18)
Q^{matter} (fm^2)	−4.07	−4.1 ±0.6	(Ref. 17)
Q^{elect} (fm^2)	−3.85	−3.8 ±1.1	(Ref. 15)
		−3.4 ±0.6	(Refs. 16 and 19)
		−3.7 ±0.08	(Ref. 20)
$\langle r^2\rangle^{\mathrm{mag}\ 1/2}$ (fm)	2.73	2.98±0.05	(Ref. 15)
μ^{mag} (μ_N)	3.38	3.256	(Ref. 16)
$\frac{\Omega^{\mathrm{mag}}}{\mu^{\mathrm{mag}}}$ (fm^2)	2.39	2.8 ±0.5	(Refs. 14 and 15)
$B(M1;\frac{3}{2}\to\frac{1}{2})$ (μ_N^2)	2.45	2.50±0.12	(Ref. 16)
$B(C2;\frac{3}{2}\to\frac{1}{2})$ (e^2fm^4)	8.04	8.3 ±0.6	(Ref. 16)
		8.3 ±0.5	(Ref. 20)

act positions the structure of the nucleons has to be taken into account.

E. Further properties of ^{7}Li

Here we discuss quantities of ^{7}Li related to the form factors. The rms charge and magnetic radii,

$$\langle r^2\rangle^{\mathrm{ch}}=\tfrac{2}{3}\langle r^2\rangle_\alpha^{\mathrm{ch}}+\tfrac{1}{3}\langle r^2\rangle_t^{\mathrm{ch}}+\tfrac{34}{147}\langle R^2\rangle\ , \tag{25}$$

$$\langle r^2\rangle^{\mathrm{mag}}=\frac{\mu_N}{\mu^{\mathrm{mag}}}\left[\tfrac{3}{14}\langle r^2\rangle_\alpha^{\mathrm{ch}}+\tfrac{4}{21}\langle r^2\rangle_t^{\mathrm{ch}}+\frac{g_t}{2}\langle r^2\rangle_t^{\mathrm{mag}}+\tfrac{1}{35}(8g_t+\tfrac{209}{98})\langle R^2\rangle\right]\ ; \tag{26}$$

the matter and electric quadrupole moments,

$$Q^{\mathrm{matter}}=-\tfrac{72}{245}\langle R^2\rangle\ , \tag{27}$$

$$Q^{\mathrm{elect}}=-\tfrac{68}{245}\langle R^2\rangle\ ; \tag{28}$$

the magnetic dipole and octupole moments,

$$\mu^{\mathrm{mag}}=\left[\frac{g_t}{2}+\frac{17}{42}\right]\mu_N\ , \tag{29}$$

$$\Omega^{\mathrm{mag}}=\tfrac{24}{245}g_t\langle R^2\rangle\mu_N\ ; \tag{30}$$

and the $M1$ and $C2$ transition probabilities to the first excited ^{7}Li* state,

$$B(M1;\tfrac{3}{2}\to\tfrac{1}{2})=\frac{1}{4\pi}(g_t-\tfrac{17}{42})^2\,|\,\langle\tilde{\psi}_{3/2}\,|\,\tilde{\psi}_{1/2}\rangle\,|^2\ , \tag{31}$$

$$B(C2;\tfrac{3}{2}\to\tfrac{1}{2})=\frac{1}{4\pi}(\tfrac{34}{49}\,|\,\langle\tilde{\psi}_{3/2}\,|\,R^2\,|\,\tilde{\psi}_{1/2}\rangle\,|\,)^2\ . \tag{32}$$

According to Sec. IV A we use the experimental values[1] for the α and t mean square radii $\langle r^2\rangle_\alpha^{\mathrm{ch}}$, $\langle r^2\rangle_t^{\mathrm{ch}}$, and $\langle r^2\rangle_t^{\mathrm{mag}}$ as an input of the elementary cluster model. Then all quantities (25)—(32) are determined by the intercluster wave functions $\psi_{3/2}$ and $\psi_{1/2}$. This cluster wave function ψ enters into most of these quantities only in the form of the expectation value $\langle R^2\rangle=\langle\tilde{\psi}_{3/2}\,|\,R^2\,|\,\tilde{\psi}_{3/2}\rangle$ which is given in Table I for the choice (12). The transition probabilities depend of course on the ^{7}Li* state via the matrix element $\langle\tilde{\psi}_{3/2}\,|\,R^2\,|\,\tilde{\psi}_{1/2}\rangle=14.49$ fm^2 and via the overlap $\langle\tilde{\psi}_{3/2}\,|\,\tilde{\psi}_{1/2}\rangle=0.998$. The overlap is almost equal to 1 because the spin orbit interaction has only a minor effect on the relative motion wave function.

In Table III the experimental values are compared to the ones calculated in the elementary cluster picture. The magnetic quantities show some deviations (up to about 10% for the magnetic rms radius), all other calculated quantities agree well with the experiment. Considering the simplicity of the model and of the resulting expressions (25)—(32), this agreement is quite satisfactory.

V. CONCLUSIONS

Most of the properties belonging to the domain of nuclear physics can be successfully described and understood in a simple cluster picture for ^{7}Li. In this sense we may conclude that the elementary cluster picture of ^{7}Li is a valid and useful model which has a similar degree of justification as the nucleon picture of the deuteron.

The elementary and the microscopic cluster picture (RGM) can be connected by identifying the intercluster wave function ψ with the RGM wave function ω (amplitude of the normalized basis states). This unique identification is enforced by the well-known formal requirements (probability amplitude) and, from the present discussion, by overwhelming evidence of calculated physical quantities.

[1]R. C. Barrett and D. F. Jackson, *Nuclear Sizes and Structure* (Clarendon, Oxford, 1977).
[2]H. Schultheis and R. Schultheis, Phys. Rev. C **25**, 2126 (1982).
[3]H. Kanada, Q. K. K. Liu, and Y. C. Tang, Phys. Rev. C **22**, 813 (1980).
[4]T. Kajino, T. Matsuse, and A. Arima, Nucl. Phys. **A413**, 323 (1984); V. K. Sharma and M. A. Nagarajan, J. Phys. G. **10**, 1703 (1984).
[5]H. Walliser, Q. K. K. Liu, H. Kanada, and Y. C. Tang, Phys. Rev. C **28**, 57 (1983).
[6]T. A. Tombrello and P. D. Parker, Phys. Rev. **131**, 2582 (1963).
[7]T. Fliessbach, Z. Phys. **A288**, 211 (1978); **A288**, 225 (1978).
[8]T. Fliessbach and P. Manakos, Nucl. Phys. **A324**, 173 (1979).
[9]T. Fliessbach, Z. Phys. **A294**, 79 (1980).
[10]Q. K. K. Liu, H. Kanada, and Y. C. Tang, Z. Phys. A **303**, 253 (1981).
[11]H. Collard, R. Hofstadter, E. B. Hughes, A. Johansson, and M. R. Yearian, Phys. Rev. **138**, B57 (1965); I. Sick, J. S. McCarthy, and R. R. Whitney, Phys. Lett. **64B**, 33 (1976).
[12]R. S. Willey, Nucl. Phys. **40**, 529 (1963).
[13]L. R. Suelzle, M. R. Yearian, and H. Crannell, Phys. Rev. **162**, 992 (1967).
[14]R. E. Rand, R. Frosch, and M. R. Yearian, Phys. Rev. **144**, 859 (1966).
[15]G. J. C. van Niftrik, L. Lapikás, H. de Vries, and G. Box, Nucl. Phys. **A174**, 173 (1971).
[16]F. Ajzenberg-Selove, Nucl. Phys. **A413**, 1 (1984).
[17]H. Orth, H. Ackermann, and E. W. Otten, Z. Phys. A **273**, 221 (1975).
[18]E. F. Gibson, J. J. Kraushaar, T. G. Masterson, R. J. Peterson, R. S. Raymond, and R. A. Ristinen, Nucl. Phys. **A377**, 389 (1982).
[19]P. Egelhof, W. Dreves, K.-H. Möbius, E. Steffens, G. Tungate, P. Zupranski, D. Fick, R. Böttger, and F. Roesel, Phys. Rev. Lett. **44**, 1380 (1980).
[20]A. Weller, P. Egelhof, R. Čaplar, O. Karban, D. Krämer, K.-H. Möbius, Z. Moroz, K. Rusek, E. Steffens, G. Tungate, K. Blatt, I. Koenig, D. Fick, submitted to Phys. Rev. Lett.